Research Article

See Kiat Wong, Liang Ee Low, Janarthanan Supramaniam, Sivakumar Manickam, Tin Wui Wong, Cheng Heng Pang*, and Siah Ying Tang*

Physical stability and rheological behavior of Pickering emulsions stabilized by protein–polysaccharide hybrid nanoconjugates

https://doi.org/10.1515/ntrev-2021-0090
received August 2, 2021; accepted September 12, 2021

Abstract: This study investigated the emulsifying properties of a protein–polysaccharide hybrid nanoconjugate system comprising cellulose nanocrystals (CNC, 1% w/v) and soy protein isolate at various concentrations (SPI, 1–3% w/v). The average particle size of the nanoconjugate increased, and the zeta potential decreased when 3% (w/v) of SPI was used. The contact angle and thermal stability of CNC improved with the conjugation of SPI. Upon Pickering emulsification, 0.5% (w/v) of CNC–SPI nanoconjugate as particle stabilizer was sufficient to obtain stable emulsions. The CNC–SPI1 formulation (CNC to SPI, 1:1) provided the emulsion with the smallest droplet size and higher emulsifying activity. Intriguingly, ultrasound (US) pre-treatment on nanoconjugates before emulsification significantly reduced the size of the emulsion. The rheological assessment demonstrated that the CNC–SPI-stabilized emulsions exhibit shear thinning behavior at a lower shear rate and shear thickening behavior at a higher shear rate, indicating the interruption of existing attractive interactions between the CNC particles. All emulsions exhibited higher elastic modulus (G') than viscous modulus (G''), suggesting high viscoelastic properties of the emulsions. This study demonstrates that CNC–SPI nanoconjugate with optimum protein to polysaccharide ratio has great potential as a natural particle stabilizer in food and nutraceutical emulsion applications.

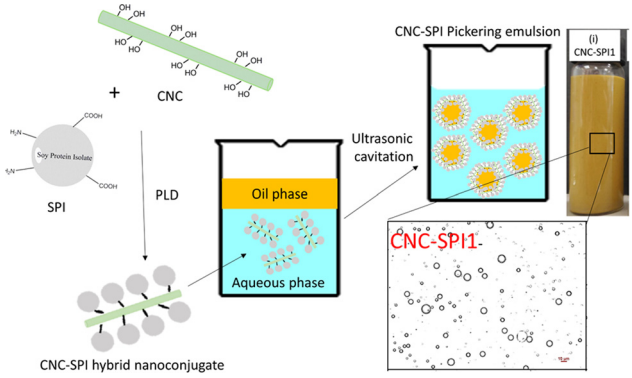

Graphical abstract

Keywords: Pickering emulsion, nanoconjugate, protein–polysaccharide, stability, rheology

*** Corresponding author: Cheng Heng Pang,** Department of Chemical and Environmental Engineering, The University of Nottingham Ningbo China, Ningbo 315100, China; New Materials Institute, The University of Nottingham Ningbo China, Ningbo 315100, China; Municipal Key Laboratory of Clean Energy Conversion Technologies, The University of Nottingham Ningbo China, Ningbo 315100, China, e-mail: ChengHeng.Pang@nottingham.edu.cn, tel: +60-3-5514-4435
*** Corresponding author: Siah Ying Tang,** Chemical Engineering Discipline, School of Engineering, Monash University Malaysia, Jalan Lagoon Selatan, Bandar Sunway, 47500 Subang Jaya, Selangor, Malaysia; Advanced Engineering Platform, Monash University Malaysia, Jalan Lagoon Selatan, Bandar Sunway, 47500 Subang Jaya, Selangor, Malaysia; Tropical Medicine and Biology Platform, School of Science, Monash University Malaysia, Jalan Lagoon Selatan, Bandar Sunway, 47500 Subang Jaya, Selangor, Malaysia, e-mail: patrick.tang@monash.edu
See Kiat Wong, Janarthanan Supramaniam: Chemical Engineering Discipline, School of Engineering, Monash University Malaysia, Jalan Lagoon Selatan, Bandar Sunway, 47500 Subang Jaya, Selangor, Malaysia
Liang Ee Low: Biofunctional Molecule Exploratory (BMEX) Research Group, School of Pharmacy, Monash University Malaysia, Jalan Lagoon Selatan, Bandar Sunway, 47500 Subang Jaya, Selangor, Malaysia; Institute of Pharmaceutics, College of Pharmaceutical Sciences, Zhejiang University, 866 Yuhangtang Road, Hangzhou, Zhejiang 310058, China
Sivakumar Manickam: Faculty of Engineering, Universiti Teknologi Brunei, BE1410 Bandar Seri Begawan, Brunei Darussalam
Tin Wui Wong: Non-Destructive Biomedical and Pharmaceutical Research Centre, Smart Manufacturing Research Institute, Universiti Teknologi MARA, 42300 Puncak Alam, Selangor, Malaysia

1 Introduction

An emulsion is a mixture of two or more immiscible liquids in a single system and is thermodynamically

unstable. To form a stable emulsion, surfactants are conventionally used to lower the surface tension between the two immiscible liquids. However, surfactants-stabilized emulsion often resulted in tissue irritation and cell damage, hence retarding their use in food-related applications [1]. Thus, utilizing food-grade solid particles as emulsion stabilizers has emerged as a crucial direction in food and nutraceutical industries, allowing the fabrication of solid particles-stabilized emulsions, commonly known as Pickering emulsion [2,3]. Furthermore, Pickering emulsion is outstanding against coalescence due to forming a protective physical barrier *via* the irreversible adsorption of solid particles onto the interface of the immiscible liquids [4,5].

Various particulate emulsifiers, such as graphene, silica, polysaccharide, and protein, have been extensively studied to form Pickering emulsion over the past decades [6]. Food-grade natural biopolymers such as polysaccharides and proteins have gathered more attention due to their lower human toxicity and environmental impacts than inorganic nanoparticles [7,8]. Among the employed polysaccharides (*e.g.*, alginate [9], chitosan [10,11], and cellulose [12–14]), cellulose nanocrystals (CNC) are of immense interest among food and nutraceutical technologists due to their abundant availability, biodegradability, and eco-friendliness [15,16]. However, CNC with high hydrophilic properties often suffers from poor emulsification performance, dramatically limiting its practical applications [17]. To overcome such issues, various topochemical surface modification approaches involving covalent chemistry and polymer coatings [18] have been applied to modify the surface characteristics of CNC to generate an effective Pickering emulsifier.

Surface functionalization or complexation employing natural proteins has emerged as a new technique to increase the surface hydrophobicity of particles for food emulsion stabilization [19,20]. One of the popular plant-based proteins, soy protein isolate (SPI), extracted from soybean, has been widely used as a food ingredient because of its high nutritional value and steady supply [21]. Furthermore, SPI is preferred among material scientists for the fabrication of functional particles in micro- and nano-sizes due to their excellent biocompatibility, biodegradability, and wide availability of various functional groups (–OH, $–NH_2$, –COOH, and –SH) that could be utilized for chemical crosslinking [22–24].

Studies have demonstrated that emulsion droplets stabilized by hybrid protein/polysaccharides contribute to excellent stability through their aggregation and absorption behaviors at the interface of the liquids. For instance, Sarkar *et al.* physically mixed CNC (1–3% w/v) with whey protein (1% w/v) to stabilize Pickering emulsion and found that a higher CNC content enhanced the stability of the emulsions and further delayed lipid digestion [25]. Besides, Hu *et al.* reported on improving the stability of emulsion droplets stabilized by sodium caseinate (2% w/v) when regenerated cellulose (0–2% w/v) was added [26]. Liu *et al.* successfully formed a high internal phase Pickering emulsion with an oil fraction of 0.8 using bovine serum albumin-stabilized CNC [17]. All these studies showed superior performance of physically mixed polysaccharide/protein as an emulsion stabilizer. Nonetheless, the performance of Pickering stabilizing of chemically bonded polysaccharide/protein remains poorly documented. To the best of our knowledge, no study has been conducted to unravel the physical and rheological properties of Pickering emulsion stabilized by CNC–SPI hybrid nanoconjugates.

This study investigates the physical, colloidal, and rheological properties of CNC–SPI hybrid nanoconjugates-stabilized Pickering emulsions in the above context. The CNC–SPI hybrid nanoconjugate was synthesized *via* a bioinspired approach using 3,4-dihydroxy-DL-phenylalanine as the linker. The present study intends to reveal the ideal protein to polysaccharide ratio of the nanoconjugate, which would improve the stability and rheological properties of the resultant Pickering emulsions. Such findings would be significant in offering new insights and knowledge toward the design and construction of biocompatible and stable protein/polysaccharide-based Pickering emulsion for food and nutraceutical applications.

2 Experimental methods

2.1 Chemicals and materials

CNC (Freeze-dried, 0.96% [w/v] of sulfur content) were procured from the University of Maine, United States. SPI was provided by Shandong Wonderful Industrial Group Co., Ltd (Shandong, China). L-Dopa, *N*-hydroxysuccinimide (NHS, 98%), *N*-(3-dimethylaminopropyl)-*N*′-ethylcarbodiimide hydrochloride (EDC, 98%) were purchased from Sigma Chemicals Co. (St. Louis, MO, USA). Red palm superolein (275 ppm β-carotene, melting point 19°C) was acquired from Sime Darby Jomalina Sdn. Bhd., Malaysia. Ultrapure water (18.2 MΩ/cm), obtained using the Milli-Q® Plus apparatus (Millipore, Billerica, USA), was used in all the experiments.

2.2 Synthesis of CNC–SPI nanoconjugates

1% w/v of CNC and 1% w/v of L-dopa were first dispersed in Tris-HCl solution at pH 8.5. The mixture was magnetically stirred at 700 rpm for 12 h at 40°C to form poly(L-dopa) (PLD) on the CNC surfaces. The resultant CNC-PLD was purified by dialyzing against deionized water for two days and freeze-dried. Then, CNC-PLD, EDC, and NHS at 1:10:10 ratio were added into 2-(*N*-morpholino)ethanesulfonic acid (MES) buffer to activate the carboxyl groups. The mixture was magnetically stirred at 700 rpm for 4 h at 25°C. The resultant CNC-PLD-NHS was purified by washing with 50% of ethanol twice and centrifuged, and the pellet was freeze-dried. 1% w/v of CNC-PLD-NHS and 1–3% w/v of SPI were dispersed in 3% w/v of *N*,*N*-diisopropylethylamine solution. The resulting mixture was magnetically stirred at 700 rpm for 24 h at 25°C. The resultant CNC-PLD-SPI was purified by washing with 80% of ethanol twice and centrifuged. The pellet was freeze-dried and kept for further analysis. For simplification, CNC-PLD-SPI will be referred to as CNC–SPI in this work. Four CNC–SPI nanoconjugates were synthesized using CNC to SPI ratios of 1:1, 1:1.5, 1:2, and 1:3 denoted as CNC–SPI1, CNC–SPI1.5, CNC–SPI2, and CNC–SPI3, respectively.

2.3 Preparation of Pickering emulsions

Pickering emulsions were prepared using the as-synthesized CNC–SPI nanoconjugate as solid stabilizers with red palm olein as the dispersed oil phase and deionized water as the continuous aqueous phase. Emulsions were prepared by mixing 20% (v/v) of palm olein with aqueous suspensions of 0.5% (w/v) of CNC–SPI nanoconjugate at pH 7, adjusted by 1 M of HCl and 1 M of NaOH. Subsequently, the mixture was emulsified using an ultrasonic horn at 60 W, 20 kHz, and 20 pulse cycles for 5 min. The freshly prepared emulsion was stored in glass vials for further analysis.

2.4 Physicochemical characterization

2.4.1 Attenuated total reflectance Fourier transform infrared (ATR-FTIR)

The molecular spectroscopy of the CNC–SPI nanoconjugates, CNC, and SPI was examined through ATR-FTIR in the frequency range of 400–4,000/cm, using FTIR spectrometer (Nicolet iS10, Thermo Scientific, USA).

2.4.2 Bradford assay

The SPI contents and conjugation efficiency were determined by the Bradford assay method. Bovine serum albumin was used as the standard. First, a known amount of CNC–SPI nanoconjugates was dissolved in 1 mL of DMSO. Ten microliter sample was then added with 1 mL of Bradford reagent (Bio-Rad, USA) and mixed thoroughly. The SPI content was determined spectrophotometrically at 595 nm after 5 min at 25°C in the dark. Triplicates were conducted for each sample, and the results were averaged. The conjugation efficiency and conjugation content were determined by employing the following equations (1) and (2):

$$\text{Conjugation efficiency (\%)} = \frac{\text{Weight of SPI in the nanoconjugate}}{\text{Weight of used SPI}} \times 100\%, \quad (1)$$

$$\text{Conjugation content (\%)} = \frac{\text{Weight of SPI in the nanoconjugate}}{\text{Weight of nanoconjugate}} \times 100\%. \quad (2)$$

2.4.3 Size and zeta potential

The average particle size and zeta potential of the CNC–SPI nanoconjugates, CNC, and SPI samples were measured using dynamic light scattering and Laser Doppler microelectrophoresis techniques, respectively, (Zetasizer Nano, Malvern Instruments, UK) at pH 7.5 and 25°C. Triplicates were conducted for each sample, and the results were averaged.

2.4.4 Thermal analysis (TGA)

The thermal profile of the CNC–SPI nanoconjugates, CNC, and SPI was assessed using a thermogravimetric analyzer (Q50 TGA, TA Instrument, USA) in the range of 25–900°C at a heating rate of 10°C/min in N_2 atmosphere. Triplicates were conducted for each sample, and the results were averaged.

2.4.5 Contact angle

The surface wettability (contact angle, $\theta_{\text{air-water}}$) of the CNC–SPI nanoconjugates, CNC, and SPI was measured

via the sessile drop method using a contact angle goniometer (Ramé-hart, Ramé-hart Instrument, USA) at 25°C. The samples were dispersed in deionized water and sonicated for 5 min before transforming into films by casting onto glass slides and dried overnight in an oven at 60°C. Seven replicates were performed for each sample, and the results were averaged.

2.4.6 Droplet size and zeta potential of Pickering emulsions

The zeta potential of Pickering emulsion was reflected by characterizing the surface charges of emulsion droplets using the Laser Doppler micro-electrophoresis technique (Zetasizer Nano, Malvern Instruments, UK) at 25°C. The average droplet size of the freshly prepared emulsions was measured using a Mastersizer (Mastersizer 3000, Malvern Instruments, UK) equipped with a Hydro EV wet dispersion unit. Average droplet size measurement was reported as volume-average diameter ($d_{4,3}$) from the particle size distribution. The average and standard deviations were calculated on five measurements with triplicate samples. Triplicates were conducted for each sample, and the results were averaged. For the storage stability study, the emulsion droplet size and visual observation were taken on days 0 and 30.

2.4.7 Visualization and localization of Pickering emulsion droplet

The size and morphology of CNC–SPI-stabilized Pickering emulsions were observed using an inverted optical microscope (Nikon Eclipse TS100, Nikon Instruments Inc., USA) at 20× magnification. The CNC–SPI nanoconjugates at the oil/water (O/W) interface were checked using an upright fluorescent microscope (Nikon Eclipse 90i, Nikon Instruments Inc., USA). One milliliter of emulsion was added with 80 μL of 0.1% of Nile blue (protein staining dye) and 0.01% of Nile red (oil staining dye) and mixed gently. The emulsion was diluted and immediately observed under the microscope. Samples were excited with laser beams at 514 nm for the Nile red and 633 nm for the Nile blue.

2.4.8 Emulsifying activity index (EAI) and emulsion stability index (ESI)

EAI and ESI were determined by the turbidimetric method with minor modification [27]. First, 0.1 mL of emulsion was diluted with 0.1% (w/v) of sodium dodecyl sulfate (SDS) solution at a ratio of 1:100 (v/v). After vortexed for 10 s, the absorbance of the diluted emulsion was determined at 500 nm using a UV-Vis spectrophotometer (Genesys 10S UV, Thermo Fisher Scientific, USA) immediately against a blank SDS solution (0.1% w/v of SDS). The EAI and ESI values were calculated using the following equations (3) and (4), respectively:

$$\mathrm{EAI}\left(\frac{\mathrm{m}^2}{\mathrm{g}}\right) = \frac{2 \times\ 2.303 \times A_0 \times N}{c \times\ \Phi \times L \times 10{,}000}, \tag{3}$$

$$\mathrm{ESI\,(min)} = \frac{A_0}{A_0\ -\ A_{10}} \times t, \tag{4}$$

where N is the dilution factor, c is the protein concentration (g/m^3), Φ is the oil volume fraction (v/v) in the emulsion, L is the optical path length (1 cm), A_0 and A_{10} are the absorbance of the diluted emulsions at 0 and 10 min, respectively, and t is the time (10 min). Measurements were performed in triplicates.

2.4.9 Rheological properties

The viscosity and viscoelastic properties of Pickering emulsions were measured using small amplitude oscillatory measurements with MCR 102 rheometer (Anton Paar Co., Austria) which is equipped with a double gap measuring system. The apparent viscosity of the emulsions was analyzed at the shear rates of 1–100/s. For the viscoelasticity properties, a range of experiments including an amplitude sweep with the shear rates of 0.1–10 Pa (frequency = 0.5 Hz) and frequency sweep of 0.1–10 Hz (strain = 0.1%) were carried out at 25°C. The measurements were performed within the linear viscoelastic region of the Pickering emulsions.

3 Results and discussion

3.1 Synthesis of CNC–SPI nanoconjugates as Pickering stabilizer

CNC–SPI nanoconjugates with different CNC to SPI ratios were synthesized according to synthesis routes shown in Figure 1. L-Dopa was utilized to crosslink the surface hydroxyl groups of CNC with the amino groups of SPI, forming CNC–SPI nanoconjugate. The solution color gradually changed from colorless to black, demonstrating

the polymerization of L-dopa into poly(L-dopa) on the CNC surface under a weak alkaline environment. Furthermore, carbodiimide chemistry involving NHS/EDC coupling reagent was used to activate the poly(L-dopa) carboxyl groups on the CNC surface, facilitating direct amidation with SPI [28]. In-depth characterization of the formed CNC–SPI nanoconjugate can be obtained from our previous study [29].

FTIR was employed to determine the chemical components of the obtained CNC–SPI nanoconjugates. Typical spectral peaks at 1,054 and 1,028/cm were recognized as the C–H stretching of CNC, and the absorption bands in the region of 3,100–3,500/cm were attributed to the O–H stretching vibrations of CNC [30]. Following conjugation with SPI, two distinctive peaks appearing at 1,626, and 1,532/cm were ascribed to the C═O stretching of amide I and N–H bending of Amide II [31], respectively, as shown in Figure 2a. CNC conjugation with a different weight ratio of SPI further led to new peaks over 1,530–1,630/cm, reflecting the prominent peak for SPI (Figure 2b). Notably, the intensity of the peaks increased as the weight ratio of SPI increased in the formulations, while the typical peaks of CNC remained the same.

The SPI content and conjugation efficiency were then determined using the Bradford assay (Figure 2c). The observed results exhibit that the SPI concentration increased from 38.22 ± 1.21 to 60.80 ± 3.37% as the weight ratio of SPI changed from 1 to 3% (w/v). It was deduced that the amount of SPI that could conjugate on the surface of CNC is controlled by the availability of vacancy sites (free activated carboxyl groups on poly(L-dopa)). When a higher concentration of SPI was used, the amount of vacancy becomes limited, thus reducing the conjugation efficiency. On the contrary, the conjugation efficiency reduced from 76.45 ± 2.78 to 40.53 ± 2.60% upon increasing the SPI content, which could be due to the insufficient anchoring sites on the CNC template for higher SPI conjugation. Nevertheless, these results indicate successful bio-inspired conjugation of SPI on the CNC surface with the assistance of an L-dopa linker.

3.2 Physicochemical properties of CNC–SPI nanoconjugates as Pickering stabilizer

The average particle size and zeta potential of the as-synthesized CNC–SPI nanoconjugates are shown in Figure 3a. The CNC particle size increased tremendously with the conjugation of SPI. The average particle size of the nanoconjugates increased from 309.97 ± 8.04 to 339.57 ± 10.89 nm

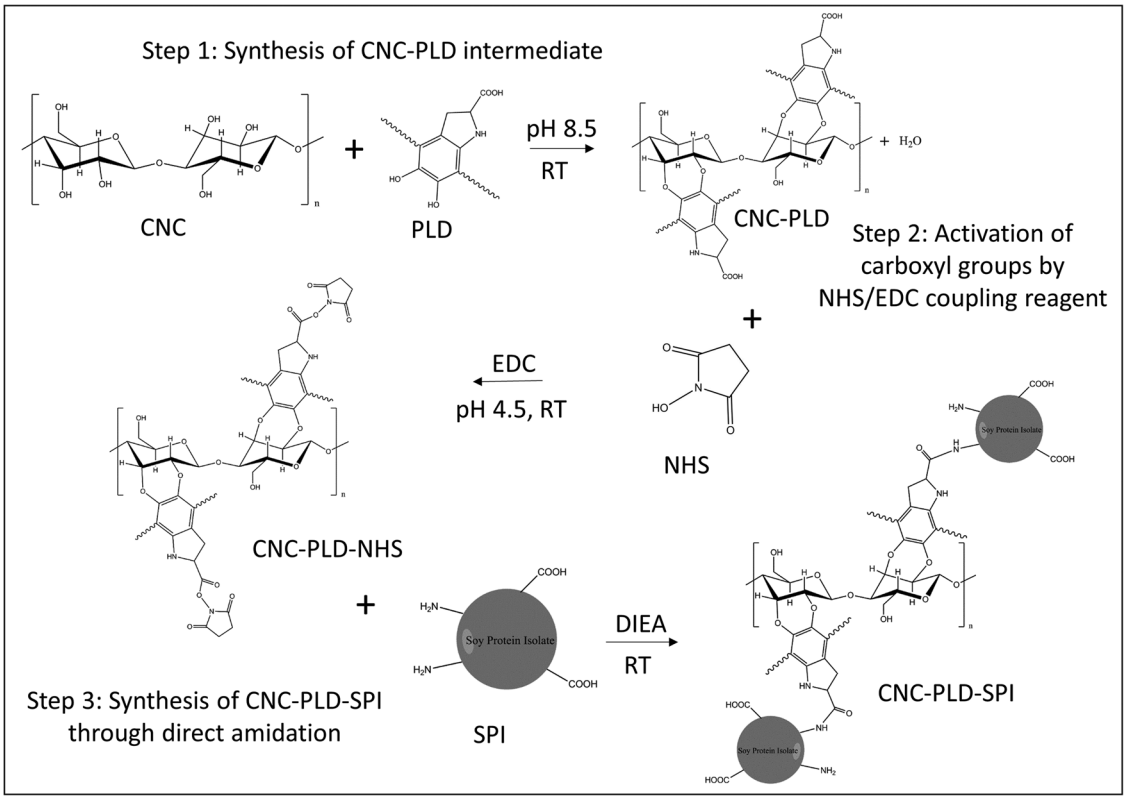

Figure 1: Synthetic routes of CNC–SPI nanoconjugates using poly(L-dopa) as a linker and NHS/EDC as the coupling reagent.

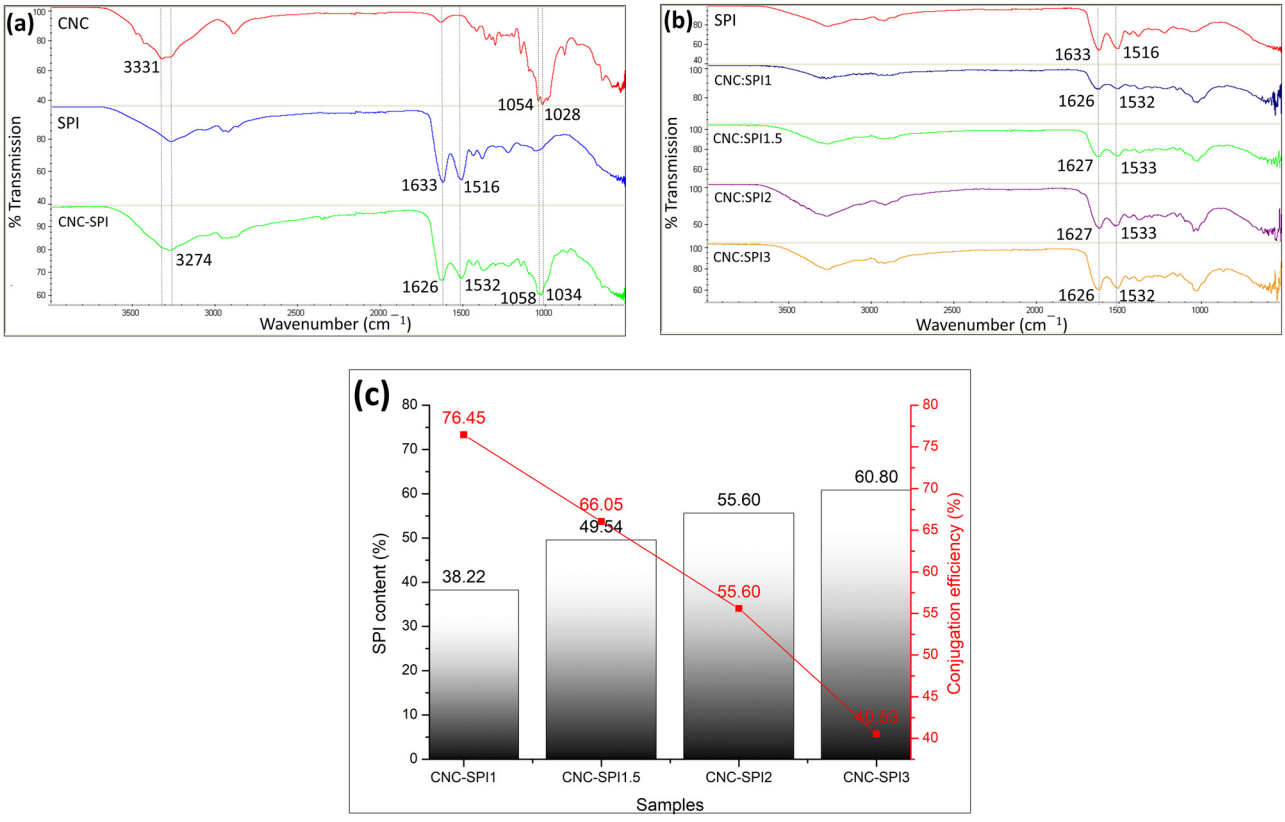

Figure 2: FTIR spectra of (a) CNC, SPI, and CNC–SPI nanoconjugate, (b) SPI, CNC–SPI1, CNC–SPI1.5, CNC–SPI2, and CNC–SPI3, and (c) SPI content and conjugation efficiency of CNC–SPI1, CNC–SPI1.5, CNC–SPI2, and CNC–SPI3 determined by the Bradford assay. Error bars represent the standard error of measurement.

upon increasing the SPI content from 1 to 3% (w/v). On the other hand, the zeta potential for CNC and SPI were −40.73 ± 1.82 and −22.03 ± 0.31 mV, respectively. CNC is an anionic polysaccharide with abundant hydroxyl groups on its surface, providing highly negative charges [32]. The net zeta potential of CNC–SPI nanoconjugate reduced with an increase in the SPI content. Thus, it can be inferred that poly(L-dopa) molecules would absorb onto the CNC surface by linking with the hydroxyl groups and then conjugate with SPI, favoring the reduction in zeta potential for better interfacial adsorption upon stabilizing Pickering emulsion.

To evaluate the influence of SPI immobilization on the wettability of CNC, water contact angle on casted sample dispersion was performed using the sessile drop method. The continuous and dispersed phases should partially wet the particles used for stabilizing the Pickering emulsion. Still, they should not be completely dissolved in any phases [33,34]. The most substantial adsorption of particles occurs when the contact angle is near 90° for the Pickering emulsion to reach the highest stability [6]. As shown in Figure 3b, the attachment of SPI to the CNC surface led to a higher water contact angle, indicating the increased hydrophobicity of CNC after modifying protein. However, with a further increase in the SPI content (CNC–SPI2 and CNC–SPI3), the water contact angle declined slightly due to the hydrophobic nature of SPI, reducing the aqueous dispersibility of CNC–SPI nanoconjugate at higher content of SPI. This causes difficulty forming a highly homogenized dispersion into a casted film, leading to a slight drop in the water contact angle. The contact angle of CNC–SPI1.5 nanoconjugate exhibited the most suitable wettability (63.7° ± 1.3°) as a Pickering stabilizer among the tested formulations.

The thermal stability of CNC–SPI nanoconjugates, CNC, and SPI was evaluated by TGA (Figure 3c). All the samples present a similar behavior with two main stages of mass loss: removing adsorbed and bound water at 80–120°C and the main thermal decomposition stage in the range of 200–350°C. Generally, the thermal stability of CNC–SPI nanoconjugate with different SPI content was enhanced compared to the unmodified CNC. The temperature contributing to 50% weight loss for unmodified CNC increased from 297 to 331°C after the addition of

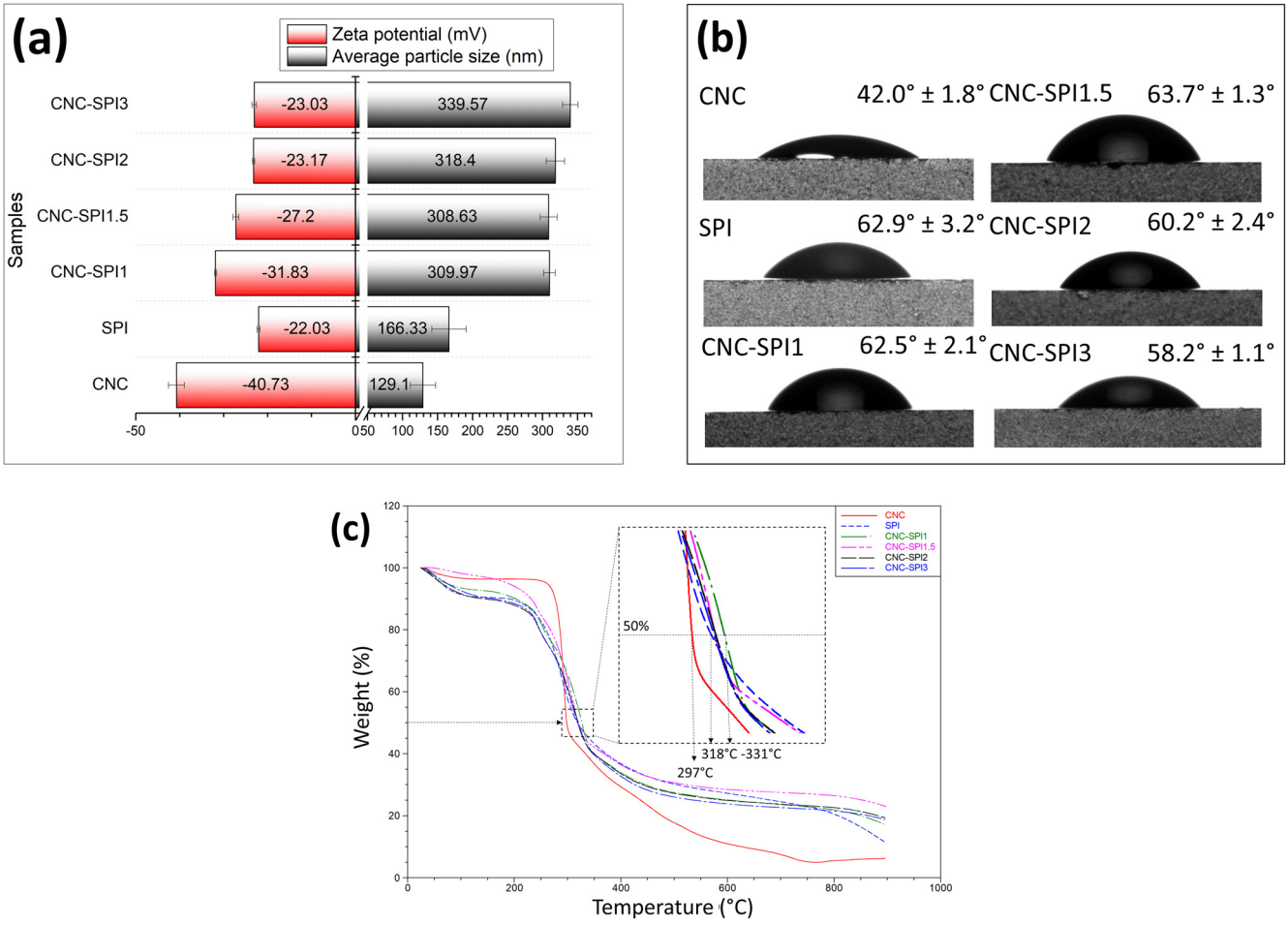

Figure 3: (a) Average particle size and zeta potential, (b) water contact angle, and (c) TGA thermograms of CNC, SPI, CNC–SPI1, CNC–SPI1.5, CNC–SPI2, and CNC–SPI3. The error bars represent the standard error of measurement.

SPI. The residual mass was more remarkable in CNC–SPI nanoconjugates, which suggests that the presence of SPI leads to the formation of a more stable protein–polysaccharide network. The improved thermal stability can be explained due to the robust polymerization of the aromatic structure of PLD followed by the conjugation of SPI on the surface of CNC [35]. However, considering the thermogravimetric profiles of all the CNC–SPI nanoconjugates, it can be stated that the thermal stability of the nanoconjugates has negligible influence on different SPI contents.

3.3 Localization and emulsification properties of CNC–SPI nanoconjugates

The localization of CNC–SPI nanoconjugates at the O/W interface was determined using fluorescent microscopy. As shown in Figure 4, the samples were prepared by the double staining method: Nile red was used to stain the red palm olein, while Nile blue was utilized for staining the nanoconjugates. The double staining method assists in differentiating the oil phase and the nanoconjugates in the emulsion system. The oil phase and CNC–SPI were visualized in the red and blue halo, respectively. The combined image uncovered the nanoconjugates around the red palm olein in the O/W Pickering emulsion. To evaluate the emulsifying ability of the as-synthesized CNC–SPI nanoconjugates, CNC nanoconjugates with different SPI content were used to form the Pickering emulsions. As described using the percentage conjugation efficiency, the content and surface coverage of CNC by SPI was distinct, resulting in different surface charges and partial wettability, ultimately affecting the emulsifying properties of the nanoconjugates.

Besides, before emulsification, ultrasound (US) pretreatment was performed on the CNC–SPI nanoconjugates to distribute the nanoconjugates evenly in the

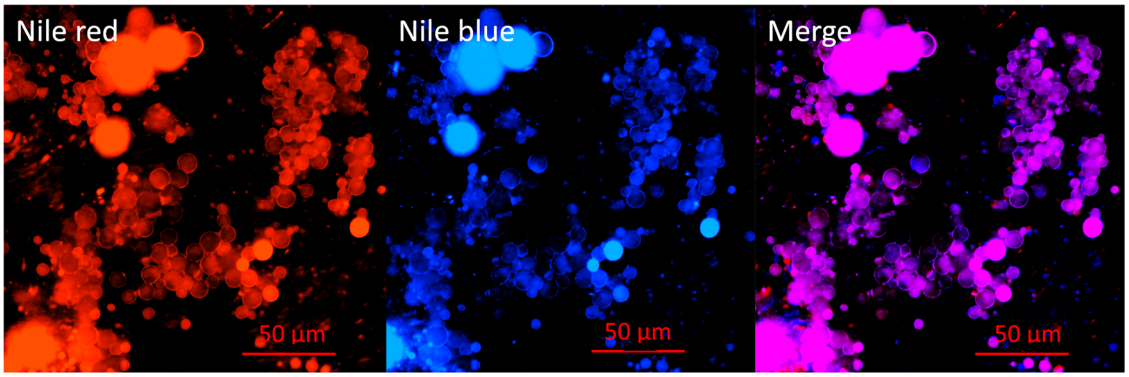

Figure 4: Fluorescent micrographs of O/W Pickering emulsion stabilized by CNC–SPI nanoconjugates with double staining. The scale bar corresponds to 50 µm.

aqueous phase to achieve the greatest emulsification performance as a Pickering stabilizer. Figure 5a and b demonstrates the droplet size distribution plot of the CNC–SPI-stabilized Pickering emulsions formed without and with 30 s US treatment, respectively, and their corresponding photographs are shown in Figure 5c and d. Based on the observation, CNC–SPI1 and CNC–SPI1.5 nanoconjugates could form homogenized emulsion droplets even without US treatment, and emulsion stabilized by CNC–SPI1 displayed a unimodal distribution of droplet size. In contrast, the emulsions stabilized by CNC–SPI2 and CNC–SPI3 nanoconjugates possess larger droplets and exhibit slight creaming (Figure 5c). Nevertheless, the emulsions stabilized by all the CNC–SPI nanoconjugates were improved with better homogeneity in the presence of US pre-treatment (Figure 5d).

Furthermore, US application also increased the functional properties of SPI by decreasing its particle size and increasing its surface hydrophobicity, resulting in improved emulsifying performance [36]. Proteins are usually large macromolecules with folded regions that hold amphiphilic properties, boosting the interfacial adsorption at multiple contact points [37]. The unfolding of proteins using US may increase the exposure of the conjugated proteins in the emulsion system, thereby favoring the formation of Pickering emulsion droplets with stronger adsorption of particles.

The differences in the average droplet size produced with and without US pre-treatments are shown in Figure 5e. Generally, the obtained droplet size is significantly smaller for Pickering emulsions generated with US pre-treatment than those prepared without US pre-treatment. The US pre-treatment aids to better disperse the nanoconjugates in the continuous phase and minimize self-aggregation. Hence, the well-dispersed CNC–SPIs attach to the O/W interphase, forming the highly stable Pickering emulsions with better interfacial particle distribution. For emulsions stabilized by CNC–SPI1, the smaller average size of 5.58 ± 2.59 µm was achieved with US pre-treatment as compared to that prepared without US pre-treatment (23.13 ± 2.17 µm). The zeta potential values of the emulsion stabilized by different CNC–SPI nanoconjugates were slightly changed, ranging from −28.45 ± 1.11 to −33.12 ± 0.51 mV for CNC–SPI3 and CNC–SPI1. The optical micrographs in Figure 5g display the morphology and droplet size of the formed emulsion droplets. Compared to the uniformly dispersed Pickering emulsions prepared using CNC–SPI with a lower SPI ratio, the Pickering emulsions formed by CNC–SPI2 and CNC–SPI3 exhibit droplets aggregation and coalescence. In addition, the degree of droplets agglomeration increased without US pre-treatment, resulting in the elevated average droplet size as obtained from Mastersizer analysis. The smallest emulsion droplets were observed in the current study when US pre-treated CNC–SPI1 was employed as the Pickering emulsion stabilizer.

As shown in Figure 5h, the emulsions stabilized by CNC–SPI1 and CNC–SPI1.5 exhibited the best stability with insignificant changes in droplet size compared to emulsions stabilized by CNC–SPI2 and CNC–SPI3 throughout the storage of 30 days. On the other hand, emulsions stabilized with higher SPI ratios also demonstrated phase separation at day 30 (Figure 5i). The increase in droplet size was primarily due to the coalescence of smaller droplets into larger droplets, as evidenced by the multimodal distribution plots for emulsions stabilized by CNC–SPI2 and CNC–SPI3 (Figure 5b). The droplets coalescence resulted in merged larger droplets rise to the top of the emulsion and being separated by the continuous phase.

To further evaluate the emulsifying properties of CNC–SPI nanoconjugates at the O/W interface, the emulsifying activity of the colloidal particles was investigated by measuring the EAI and ESI, as shown in Table 1. The

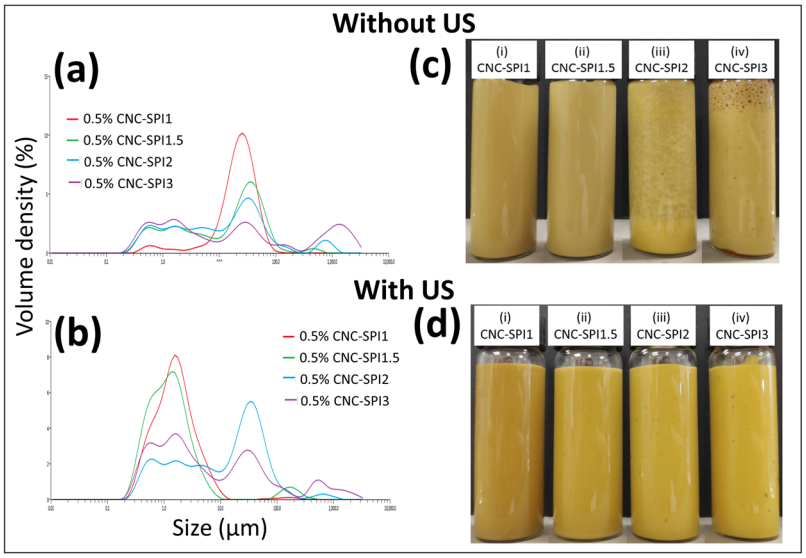

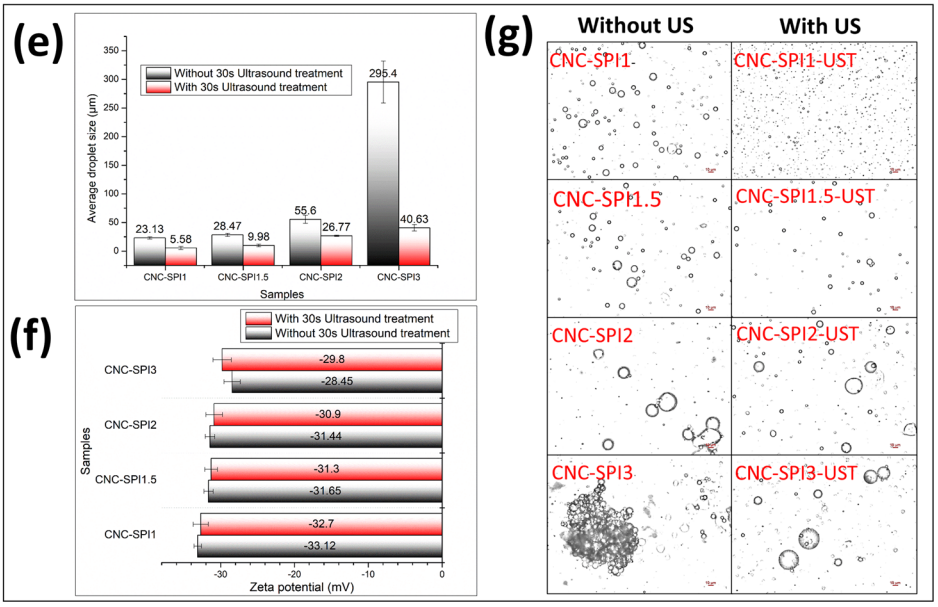

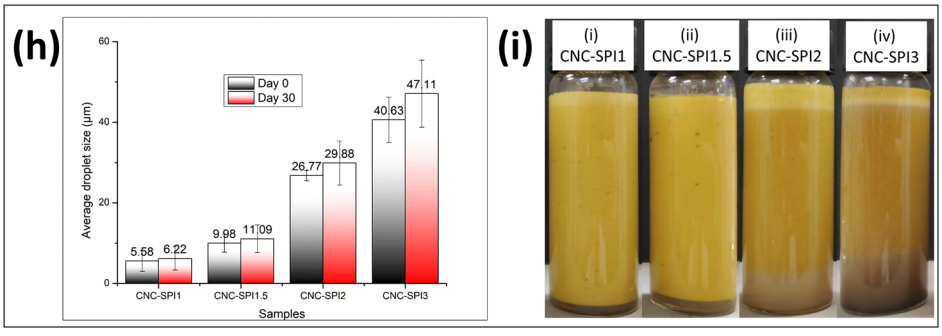

Figure 5: Droplet size distribution of the Pickering emulsions formed (a) without ultrasound treatment, (b) with ultrasound treatment before emulsification and visual observations, (c) without ultrasound treatment, (d) with ultrasound treatment before emulsification, (e) average droplet size, $d_{4,3}$ values, (f) zeta potential, (g) optical micrographs of the Pickering emulsion stabilized by CNC–SPI nanoconjugates, (h) average droplet size, $d_{4,3}$ values, and (i) visual observation of emulsions at days 0 and 30. The error bars represent the standard error of measurement.

Table 1: : The emulsifying properties (EAI and ESI) for the emulsions stabilized by CNC, SPI, and CNC–SPI nanoconjugates

Samples	EAI (m^2/g)	ESI (min)
CNC	122.4 ± 16.9	105.3 ± 11.9
SPI	100.4 ± 4.8	98.4 ± 9.5
CNC–SPI1	180.3 ± 8.9	154.4 ± 21.8
CNC–SPI1.5	162.3 ± 6.8	137.9 ± 24.7
CNC–SPI2	151.4 ± 4.0	128.7 ± 10.1
CNC–SPI3	140.4 ± 7.8	117.9 ± 2.1

EAI values of the emulsions stabilized by CNC, SPI, and CNC–SPI1 were 122.4 ± 16.9, 100.4 ± 4.8, and 180.3 ± 8.9, respectively, indicating a drastic improvement in the emulsifying activity of CNC with the conjugation of hydrophobic protein. Similar results were obtained by Dong *et al.*, where the emulsifying activity of flaxseed gum was significantly enhanced when whey protein isolate was conjugated and used together as a hybrid polysaccharide–protein conjugate emulsifier [27]. The CNC–SPI1 exhibited the highest emulsifying activity compared to other formulations. This could be attributed to the decrease in the surface charges of CNC, lowering the electrostatic repulsion between the particles for stronger interfacial adsorption (Figure 3a) [38].

On the other hand, a similar trend was observed for ESI, where the CNC–SPI nanoconjugates displayed higher ESI values than the individual CNC and SPI. CNC–SPI1 attained the maximal ESI value, and it decreased with an increase in the SPI content. This observation agrees with the results of average particle size (Figure 3a) and the contact angles of particles (Figure 3b), whereby smaller particles with optimum wettability led to more stable emulsions. These results suggest that the 1:1 ratio of CNC to SPI is the most desired in forming stable Pickering emulsions, enabling balanced hydrophilic-lipophilic groups and promoting effective anchoring of particles at the O/W interface to improve the emulsion properties [39].

3.4 Rheological behaviors of Pickering emulsions

The rheological properties of food-based materials are very useful pre-requisites for their successful application in predicting the performance during processing and evaluating the food quality and stability. Therefore, it is crucial to study the rheological properties by measuring the dynamic viscoelasticity and steady flow behavior of the Pickering emulsions. For the steady flow test, the viscosity curves of the emulsions stabilized by CNC, SPI, and different CNC–SPI nanoconjugates are shown in Figure 6a. The CNC- and SPI- stabilized emulsions show a typical shear-thinning behavior, where the viscosity decreases as the shear rate increases. In contrast, the CNC–SPI nanoconjugates-stabilized emulsions exhibit shear thinning behavior at a low shear rate and behave like a Newtonian fluid at a higher shear rate, where shear plateau or shear thickening is observed. The shear-thinning behavior of the emulsions could be due to the weak attractive interactions between the particles (hydrogen bonds). In contrast, the turnover of the rheological behavior from shear-thinning to Newtonian behavior could be due to the disruption of the existing particle-particle network [40].

The results illustrate increased viscosity for the emulsions stabilized by CNC–SPI nanoconjugates compared to CNC-stabilized emulsions. Therefore, it can be assumed that the presence of SPI led to a more robust floc structure, reducing the flowability, as evidenced by their larger droplet size (Figure 5e) and optical images (Figure 5g). It is deduced that smaller emulsion droplets with higher viscosity could reduce the phase partition by minimizing the gravitational separation rate when CNC–SPI hybrid particles are used as stabilizers [39]. Angkuratipakorn *et al.* reported similar findings where adding 2.5% of gum Arabic in CNC/surfactants-stabilized emulsions resulted in an enhanced apparent viscosity at high shear rates [41]. This suggests that SPI moieties on CNC nanoconjugates-stabilized emulsions would give rise to the formation of a stronger gel network, which slows down the movement of the droplets.

The viscoelasticity profiles of Pickering emulsions stabilized by CNC–SPI nanoconjugates demonstrated by oscillatory stress sweep and frequency sweep are shown in Figure 6b and c, respectively. For all the emulsions, the elastic modulus (G') is always larger than the viscous modulus (G'') at lower amplitudes, similar to the finding where a hybrid protein–polysaccharide emulsifier was used [42]. A crossover point between G' and G'' could be observed as the amplitude increases, indicating the rearrangement of emulsion droplets forming a percolating network structure. The emulsion stabilized by pure CNC displayed the crossover point at the lowest amplitude compared to the rest of the emulsions, demonstrating improved viscoelastic behavior when CNC–SPI nanoconjugates were used (Figure 6b). This can be explained by the higher viscous properties of protein–polysaccharide complexes or coacervates than the CNC linear polysaccharide [41], enabling the formation of emulsions with typical gel-like behavior and considerably enhanced stability.

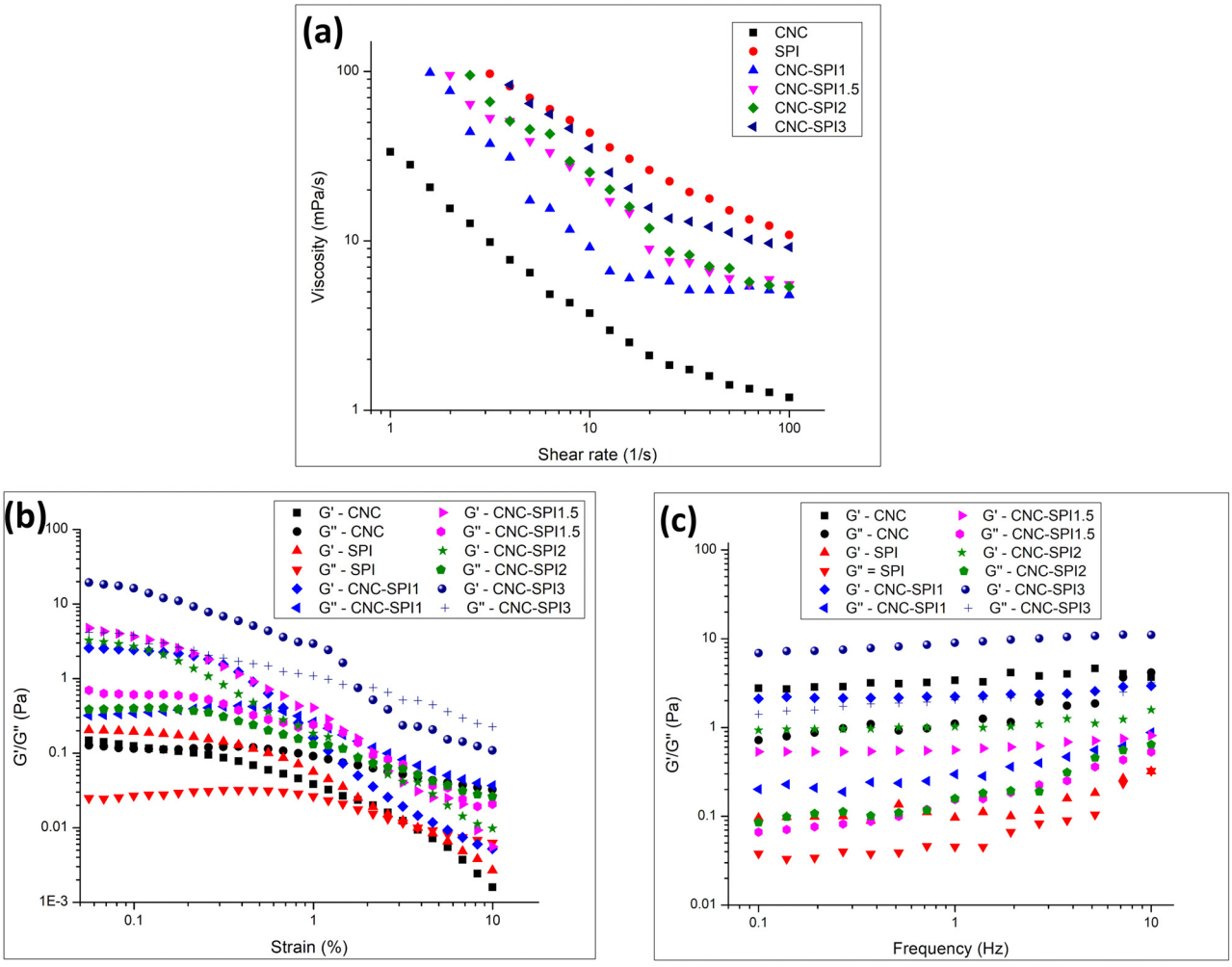

Figure 6: (a) Viscosity for the O/W emulsions stabilized by CNC, SPI, and CNC–SPI nanoconjugates as a function of shear rate. The *G′* and *G″* for the O/W emulsions stabilized by CNC, SPI, and CNC–SPI nanoconjugates as a function of (b) shear strain and (c) frequency.

On the other hand, Figure 6c shows that all the emulsions exhibited higher storage modulus (*G′*) than loss modulus (*G″*), and both moduli are nearly independent on frequency (0.1–10 Hz), suggesting a high elasticity of the solution. There is no crossover point between *G′* and *G″* as a function of frequency for all the emulsions except for the emulsions stabilized by pure CNC and SPI. A crossover point at a frequency of around 7 Hz was observed for both the emulsions, demonstrating less elastic behavior when a single biopolymer was used as the stabilizer. Higher storage modulus could provide excellent creaming stability due to the droplet flocculation [43], higher internal rheological resistance, and emulsion stability [44]. This indicates that CNC–SPI nanoconjugates can be absorbed in the O/W interface to favor forming a 3-D network structure with enhanced interfacial viscoelasticity.

Similarly, CNC–SPI nanoconjugates with the highest SPI content exhibited the most significant increment in the storage modulus, indicating a greater solid-like structure. Materials with a higher storage modulus have a stronger recovery force, thus, having more resistance against deformation [42]. This could be due to the lower surface repulsive force between the materials expressed by the lower zeta potential (Figure 3a). Thus, the choice of stabilizer with different protein to polysaccharide ratios would be critical to generate O/W Pickering emulsion with the required viscoelasticity as displayed by the ratio-dependent surface properties of the nanoconjugate.

4 Conclusion

This study investigated the stability and rheological properties of Pickering emulsion stabilized by CNC–SPI nanoconjugates with different SPI contents. The conjugation

efficiency of SPI onto CNC was reduced with an increase in SPI to CNC weight ratio due to the possible insufficient anchoring sites on the CNC template. It was found that the interactions between CNC and SPI increased the particle size, reduced the surface charges, increased the surface hydrophobicity, and improved the thermal stability of the nanoconjugates compared to pristine CNC. The Pickering emulsions stabilized by CNC–SPI1 displayed higher physical stability, with monomodal size distribution and enhanced emulsifying activity indicated by higher EAI and ESI values. Before emulsification, the US pre-treatment on the nanoconjugates also significantly reduced the size of resultant Pickering emulsions to better-dispersed nanoconjugates in the continuous phase and minimized self-aggregation. For the rheological assessment, emulsions stabilized with CNC–SPI nanoconjugates with the highest SPI content showed the highest viscosity, and the viscosity decreased with an increased shear rate. In addition, all the emulsions exhibited higher storage modulus (G') than loss modulus (G''), indicating the high elastic properties of emulsions, resulting in higher emulsion stability. A proper SPI to CNC ratio as the stabilizer is crucial for forming emulsion to obtain the desired viscoelastic characteristics. An in-depth study about the molecular interaction of CNC and SPI on the liquid–liquid interface could be explored further to demonstrate the efficacy of using a stabilizer with combined biopolymers. This study provides valuable information on the physical stability and rheological properties of Pickering emulsions stabilized by the hybrid protein–polysaccharide nanoconjugate system. It is believed that it may be applied to improve the quality of relevant emulsion products.

Acknowledgement: The authors gratefully express gratitude to all parties who have contributed towards the success of this project, both financially and technically, especially the S&T Innovation 2025 Major Special Programme (grant number 2018B10022) and the Ningbo Natural Science Foundation Programme (grant number 2018A610069) funded by the Ningbo Science and Technology Bureau, China, as well as the UNNC FoSE Faculty Inspiration Grant, China. The Zhejiang Provincial Department of Science and Technology is also acknowledged for this research under its Provincial Key Laboratory Programme (2020E10018). This project was supported by the Tropical Medicine and Biology Platform, School of Science, Monash University Malaysia.

Funding information: The S&T Innovation 2025 Major Special Programme (grant number 2018B10022) and the Ningbo Natural Science Foundation Programme (grant number 2018A610069) funded by the Ningbo Science and Technology Bureau, China, as well as the UNNC FoSE Faculty Inspiration Grant, China. The Zhejiang Provincial Department of Science and Technology is also acknowledged for this research under its Provincial Key Laboratory Programme (2020E10018). This project was supported by the Tropical Medicine and Biology Platform, School of Science, Monash University Malaysia.

Author contributions: All authors have accepted responsibility for the entire content of this manuscript and approved its submission.

Conflict of interest: The authors declare no conflict of interest.

References

[1] Tang J, Quinlan PJ, Tam KC. Stimuli-responsive Pickering emulsions: recent advances and potential applications. Soft Matter. 2015;11(18):3512–29.
[2] Ramsden W. Separation of solids in the surface-layers of solutions and 'suspensions' (observations on surface-membranes, bubbles, emulsions, and mechanical coagulation). – Preliminary account. Proc R Soc Lond. 1904;72(477–486):156–64.
[3] Pickering SU. Emulsions. J Chem Soc Trans. 1907;91:2001–21.
[4] Low LE, Wong SK, Tang SY, Chew CL, De Silva HA, Lee JMV, et al. Production of highly uniform Pickering emulsions by novel high-intensity ultrasonic tubular reactor (HUTR). Ultrason Sonochem. 2019;54:121–8.
[5] Low LE, Tan LTH, Goh BH, Tey BT, Ong BH, Tang SY. Magnetic cellulose nanocrystal-stabilized Pickering emulsions for enhanced bioactive release and human colon cancer therapy. Int J Biol Macromol. 2019;127:76–84.
[6] Chevalier Y, Bolzinger M-A. Emulsions stabilized with solid nanoparticles: Pickering emulsions. Colloids Surf A: Physicochem Eng Asp. 2013;439:23–34.
[7] Tavernier I, Wijaya W, Van der Meeren P, Dewettinck K, Patel AR. Food-grade particles for emulsion stabilization. Trends Food Sci Technol. 2016;50:159–74.
[8] Dickinson E. Biopolymer-based particles as stabilizing agents for emulsions and foams. Food Hydrocoll. 2017;68:219–31.
[9] Zhang W, Sun X, Fan X, Li M, He G. Pickering emulsions stabilized by hydrophobically modified alginate nanoparticles: Preparation and pH-responsive performance *in vitro*. J Dispers Sci Technol. 2018;39(3):367–74.
[10] Mwangi WW, Ho KW, Tey BT, Chan ES. Effects of environmental factors on the physical stability of pickering-emulsions stabilized by chitosan particles. Food Hydrocoll. 2016;60:543–50.
[11] Wang XY, Heuzey MC. Chitosan-based conventional and Pickering emulsions with long-term stability. Langmuir. 2016;32(4):929–36.
[12] Hu Z, Marway HS, Kasem H, Pelton R, Cranston ED. Dried and redispersible cellulose nanocrystal Pickering emulsions. ACS Macro Lett. 2016;5(2):185–9.

[13] Lu X, Zhang H, Li Y, Huang Q. Fabrication of milled cellulose particles-stabilized Pickering emulsions. Food Hydrocoll. 2018;77:427–35.
[14] Low LE, Tey BT, Ong BH, Chan ES, Tang SY. Palm olein-in-water Pickering emulsion stabilized by Fe_3O_4-cellulose nanocrystal nanocomposites and their responses to pH. Carbohydr Polym. 2017;155:391–9.
[15] Li A, Xu D, Luo L, Zhou Y, Yan W, Leng X, et al. Overview of nanocellulose as additives in paper processing and paper products. Nanotechnol Rev. 2021;10(1):264–81.
[16] Saji VS. Carbon nanostructure-based superhydrophobic surfaces and coatings. Nanotechnol Rev. 2021;10(1):518–71.
[17] Liu ZJ, Huang CH, Tang CH, Ou SY. Pickering high internal phase emulsions stabilized by protein-covered cellulose nanocrystals. Food Hydrocoll. 2018;82:96–105.
[18] Eyley S, Thielemans W. Surface modification of cellulose nanocrystals. Nanoscale. 2014;6(14):7764–79.
[19] George J, Sabapathi S. Cellulose nanocrystals: synthesis, functional properties, and applications. Nanotechnol Sci Appl. 2015;8:45.
[20] Feng Y, Lee Y. Surface modification of zein colloidal particles with sodium caseinate to stabilize oil-in-water pickering emulsion. Food Hydrocoll. 2016;56:292–302.
[21] Liu F, Tang CH. Soy protein nanoparticle aggregates as Pickering stabilizers for oil-in-water emulsions. J Agric Food Chem. 2013;61(37):8888–98.
[22] Song F, Tang DL, Wang XL, Wang YZ. Biodegradable soy protein isolate-based materials: a review. Biomacromolecules. 2011;12(10):3369–80.
[23] Ma L, Yang Y, Yao J, Shao Z, Chen X. Robust soy protein films obtained by slight chemical modification of polypeptide chains. Polym Chem. 2013;4(21):5425–31.
[24] Zhang S, Xia C, Dong Y, Yan Y, Li J, Shi SQ, et al. Soy protein isolate-based films reinforced by surface modified cellulose nanocrystal. Ind Crop Prod. 2016;80:207–13.
[25] Sarkar A, Li H, Cray D, Boxall S. Composite whey protein–cellulose nanocrystals at oil–water interface: towards delaying lipid digestion. Food Hydrocoll. 2018;77:436–44.
[26] Hu HY, Xing LJ, Hu YY, Qiao CI, Wu T, Zhou GH, et al. Effects of regenerated cellulose on oil-in-water emulsions stabilized by sodium caseinate. Food Hydrocoll. 2016;52:38–46.
[27] Dong X, Du S, Deng Q, Tang H, Yang C, Wei F, et al. Study on the antioxidant activity and emulsifying properties of flaxseed gum-whey protein isolate conjugates prepared by Maillard reaction. Int J Biol Macromol. 2020;153:1157–64.
[28] Wong SK, Zainol I, Ng MP, Ng CH, Ooi H, Dendrimer-like AB. 2-type star polymers as nanocarriers for doxorubicin delivery to breast cancer cells: synthesis, characterization, *in-vitro* release and cytotoxicity studies. J Polym Res. 2020;27(7):1–19.
[29] Wong SK, Supramaniam J, Wong TW, Soottitantawat A, Ruktanonchai UR, Tey BT, et al. Synthesis of bio-inspired cellulose nanocrystals-soy protein isolate nanoconjugate for stabilization of oil-in-water Pickering emulsions. Carbohydr Res. 2021;108336.
[30] Zaman M, Xiao H, Chibante F, Ni Y. Synthesis and characterization of cationically modified nanocrystalline cellulose. Carbohydr Polym. 2012;89(1):163–70.
[31] Li JS, Han Y, Li J, Chen H. Improvement in functional properties of soy protein isolate-based film by cellulose nanocrystal–graphene artificial nacre nanocomposite. Polymers. 2017;9(8):321.
[32] Lin N, Dufresne A. Surface chemistry, morphological analysis and properties of cellulose nanocrystals with gradiented sulfation degrees. Nanoscale. 2014;6(10):5384–93.
[33] Lv P, Wang D, Chen Y, Zhu S, Zhang J, Mao L, et al. Pickering emulsion gels stabilized by novel complex particles of high-pressure-induced WPI gel and chitosan: Fabrication, characterization and encapsulation. Food Hydrocoll. 2020;108:105992.
[34] Low LE, Siva SP, Ho YK, Chan ES, Tey BT. Recent advances of characterization techniques for the formation, physical properties and stability of Pickering emulsion. Adv Colloid Interface Sci. 2020;277:102117.
[35] Shang Q, Liu C, Hu Y, Jia P, Hu L, Zhou Y. Bio-inspired hydrophobic modification of cellulose nanocrystals with castor oil. Carbohydr Polym. 2018;191:168–75.
[36] Deng L. Current progress in the utilization of soy-based emulsifiers in food applications – a review. Foods. 2021;10(6):1354.
[37] Ashaolu TJ, Zhao G. Fabricating a pickering stabilizer from okara dietary fibre particulates by conjugating with soy protein isolate *via* maillard reaction. Foods. 2020;9(2):143.
[38] Xiong Z, Zhang M, Ma M. Emulsifying properties of ovalbumin: Improvement and mechanism by phosphorylation in the presence of sodium tripolyphosphate. Food Hydrocoll. 2016;60:29–37.
[39] Wan ZL, Wang JM, Wang LY, Yuan Y, Yang XQ. Complexation of resveratrol with soy protein and its improvement on oxidative stability of corn oil/water emulsions. Food Chem. 2014;161:324–31.
[40] Heyse A, Kraume M, Drews A. The impact of lipases on the rheological behavior of colloidal silica nanoparticle-stabilized Pickering emulsions for biocatalytical applications. Colloids Surf B: Biointerfaces. 2020;185:110580.
[41] Angkuratipakorn T, Sriprai A, Tantrawong S, Chaiyasit W, Singkhonrat J. Fabrication and characterization of rice bran oil-in-water Pickering emulsion stabilized by cellulose nanocrystals. Colloids Surf A: Physicochem Eng Asp. 2017;522:310–9.
[42] Li MF, He ZY, Li GY, Zeng QZ, Su DX, Zhang JL, et al. The formation and characterization of antioxidant pickering emulsions: effect of the interactions between gliadin and chitosan. Food Hydrocoll. 2019;90:482–9.
[43] Xiong W, Ren C, Tian M, Yang X, Li J, Li B. Emulsion stability and dilatational viscoelasticity of ovalbumin/chitosan complexes at the oil-in-water interface. Food Chem. 2018;252:181–8.
[44] Junqueira LA, Amaral TN, Leite Oliveira N, Prado MET, de Resende JV. Rheological behavior and stability of emulsions obtained from Pereskia aculeata Miller *via* different drying methods. Int J Food Prop. 2018;21(1):21–35.